Control of the chirality of spiral waves and recreation of spatial excitation patterns through optogenetics

Teng-Chao Li, Wei Zhong,* and Bao-quan Ai
Guangdong Provincial Key Laboratory of Quantum Engineering and Quantum Materials and School of Physics and Telecommunication Engineering, South China Normal University, Guangzhou 510006, China and Guangdong-Hong Kong Joint Laboratory of Quantum Matter, Frontier Research Institute for Physics, South China Normal University, Guangzhou 510006, China

Alexander V. Panfilov†
Ural Federal University, Biomed Laboratory, 620002 Ekaterinburg, Russia; Ghent University, 9000 Ghent, Belgium; and World-Class Research Center "Digital Biodesign and Personalized Healthcare," I. M. Sechenov First Moscow State Medical University, 119146 Moscow, Russia

Hans Dierckx
KU Leuven Campus Kortrijk-Kulak, Department of Mathematics, Etienne Sabbelaan 53, 8500 Kortrijk, Belgium and iSi Health - KU Leuven Institute of Physics-based Modeling for In Silico Health, KU Leuven, Belgium

(Received 14 September 2021; accepted 6 January 2022; published 25 January 2022)

Spiral waves lead to dangerous arrhythmias in the cardiac system. In 2015 Burton *et al.* demonstrated the reversal of the spiral wave chirality through the rotating spiral-shaped illumination on the optogenetically modified cardiac monolayers. We show that this process entails the recreation of a spiral wave. We show how this methodology can be used to control and create the desired spatial excitation pattern. We found that the control is sensitive to the area of illuminated region but independent of the phase difference of the existing spiral wave and the applied spiral-shaped light. We also discovered that our methodology can temporarily resynchronize a turbulent system. The results offer numerical evidence for the control of spatial pattern in biological excitable systems with optogenetics.

DOI: 10.1103/PhysRevE.105.014214

I. INTRODUCTION

Rotating spiral waves are one of the most studied nonlinear patterns that have been observed in diverse systems [1] such as the Belousov-Zhabotinsky (BZ) reaction [2], CO oxidation on platinum [3], and *Xenopus* oocyte calcium waves [4]. Currently, spiral waves attract a great deal of interest due to their association with cardiac arrhythmias [5,6], including atrial fibrillation (AF) [7] and ventricular fibrillation (VF) [8].

Chirality is a fundamental property of a spiral wave that affects the system's dynamics [9–11]. Spiral chirality can be identified by evaluating the value of the topological charge at the tip location. The topological charge is defined as

$$n_t = (1/2\pi)\oint_\Gamma \vec{\nabla}\phi \cdot d\vec{l}, \qquad (1)$$

where $\phi(x, y)$ represents the local phase, and Γ is a closed curve surrounding the tip. The elements adjacent to the tip exhibit a continuous phase distribution that is equal to $\pm 2\pi$. Consequently, the integral is equal to 1 or -1, which corresponds to a clockwise or counterclockwise rotating spiral wave. Several methods have been proposed to select the chirality of spiral waves. Quail *et al.* discovered that in an isotropic cardiac medium, the relative position between unexcitable obstacles and the pacing site may determine the chirality of a spiral wave [9]. Li *et al.* [12] found that an external circularly polarized electric field breaks the chiral symmetry of a turbulent system by selecting the spiral defects with a specific chirality. Experimental evidence was presented by Ji *et al.* [13].

The optical control of spiral waves has been studied numerically and experimentally in both chemical and biological systems. Steinbock *et al.* [14] demonstrated that in a light-sensitive BZ reaction a meandering spiral wave could be forced to rigid rotation by an argon laser beam creating an unexcitable disk close to the tip. Recently optogenetics has emerged as a potential tool which allows us to study and operate the biological systems [15]. Controlling the spiral waves in cardiac tissue through optogenetics is believed to be a possible technique for heart defibrillation [16]. Majumder *et al.* [17] showed that with light-induced blocks, the tip trajectories of the spiral wave can be positioned on the predefined pathway. Bingen *et al.* [18] showed that spiral waves in atrial cardiomyocyte monolayers can be terminated effectively by a light-induced depolarizing current. Hussaini *et al.* [19] demonstrated that the subthreshold illumination

*Corresponding author: zhong_wei@m.scnu.edu.cn
†Corresponding author: alexander.panfilov@ugent.be

on cardiac tissue lowers the rotation frequency of the spiral waves, and a suitable subthreshold illumination may cause drift or termination of spiral waves.

A method for reversing the chirality of an ongoing spiral wave through optogenetics was proposed by Burton *et al.* [20] in 2015. Specifically, they transiently imposed a computer-generated spiral-shaped light with an opposite chirality which has a slightly higher frequency of rotation compared to the native spiral. Within one or two rotation periods, the imposed wave effectively overwrites the existing spiral wave and persists after the light removal. This reversal of spiral wave chirality is independent of the phase of the ongoing spiral and is repeatable. In this paper we numerically reproduce Burton's work and investigate the mechanisms behind the reversal process. We find that the mechanism is recreation of a spiral wave. Further, we change the characteristics of the light pattern to investigate under which conditions the spiral patterns can be recreated. Numerical experiments in three cases are performed: spiral recreation using spatial offset, illumination with a spiral-pair-shaped light, and partial illumination. Also, to show the robust of the mechanisms, we investigate the effects of the illumination on different excitable systems, including the meandering spiral wave system, multiple spiral wave system, and turbulent system.

II. METHODS

A. A computational model for spiral system

We use a generic reaction-diffusion model for the excitable system:

$$\frac{\partial u}{\partial t} = D\Delta u + \varepsilon^{-1}u(1-u)[u-(v+b)/a] + I(x,y,t), \quad (2)$$

$$\frac{\partial v}{\partial t} = u - v, \quad (3)$$

where in application to cardiac tissue, the non-linear function $u(1-u)[u-(v+b)/a]$ describes an instantaneous depolarizing ionic current, and variable $v(x,y,t)$ accounts for repolarization of the membrane and thus mimics a slow repolarizing ionic current. This model is also known as the Barkley model [21]. The parameters $D=1$, $a=1.1$, $b=0.19$, and $\varepsilon=0.02$ are chosen. Using the Heaviside step function $H(t-t_0)$, the stimulation when the light is switched on can be specified by the function

$$I(x,y,t) = I_0 \cdot [\vec{r} \in \Omega(x,y,t)] \cdot H(t-t_0)H(t_0+\delta-t), \quad (4)$$

where I_0 represents the light intensity, t_0 is the time when the stimulation begins, and δ is the duration of the pulse. The rotating spiral-shaped illuminated region $\Omega(x,y,t)$ is generated by copying from an auxiliary spiral wave under the same model and parameters. We set the place where $u>0.5$ in the rotating auxiliary spiral wave as the illuminated region. The angular frequency of the spiral-shaped light is controlled by an external field, which is described in Ref. [22]. Specifically, we choose a suitable ω in the expression of $\mathbf{E}$ in Eq. (1) of Ref. [22] to tune the frequency of the auxiliary spiral wave.

Numerical simulations are performed on a squared medium of size 24×24 with zero-flux boundary conditions. We use the explicit Euler stepping method with space step $\Delta x = \Delta y = 0.2$ and time step $\Delta t = 0.005$. We take $I_0 = 0.2/\Delta t$. With the above parameters, the spiral wave will rigidly rotate with its natural angular frequency $\omega_0 = 1.245$ and rotation period $T_0 = 5.045$ in the medium.

To obtain the meandering spiral wave, we set the parameters $D=1$, $a=1.1$, $b=0.05$, and $\varepsilon=0.02$, with which one can get its natural frequency $\omega_1 = 1.387$ and the rotation period $T_1 = 4.530$ by using the software DXSPIRAL [23,24]. The illumination region $\Omega(x,y,t)$ for such case is generated by copying from a spiral synchronized by an external field [22,24] under the same model and parameters.

B. Computational models for turbulent systems

We use two models to create the turbulent state. The first model is the variant of the Barkley model [25]:

$$\frac{\partial u}{\partial t} = D\Delta u + \varepsilon^{-1}u(1-u)[u-(v+b)/a] + I(x,y,t), \quad (5)$$

$$\frac{\partial v}{\partial t} = u^3 - v. \quad (6)$$

For the excitable medium, the parameters $D=1$, $a=0.6$, $b=0.06$, and $\varepsilon=0.0875$ are chosen, with which the resonant frequency, that is, the dominate peak in the Fourier spectrum, of the turbulence is $\omega_2 = 1.020$ and the corresponding period is $T_2 = 6.160$.

The second model is the Bär model [26]:

$$\frac{\partial u}{\partial t} = D\Delta u + \varepsilon^{-1}u(1-u)[u-(v+b)/a] + I(x,y,t), \quad (7)$$

$$\frac{\partial v}{\partial t} = h(u) - v \quad (8)$$

with $h(u)=0$ if $0 \leqslant u < 1/3$; $h(u) = 1-6.75u(u-1)^2$ if $1/3 \leqslant u < 1$; and $h(u)=1$ if $1<u$. Parameters are $D=1$, $a=0.84$, $b=0.07$, and $\varepsilon=0.072$. The resonant frequency of the turbulence is $\omega_3 = 1.260$, and the corresponding period is $T_3 = 4.987$.

For the illumination, we choose the same method and parameters used as in Sec. II A.

III. RESULTS

A. Reproduction of Burton's experiments

Figure 1 shows our numerical simulation of Burton's experiments of reversing the spiral wave chirality. We start from a clockwise rigidly rotating spiral wave whose tip locates in the center of the medium as depicted in Fig. 1(a). The counterclockwise rotating spiral-shaped light locates in the center as well. Figure 1(b) shows that shortly after the illumination begins, two spiral patterns exist in the medium. As the illumination continues, the contour of the clockwise spiral wave becomes illegible in Fig. 1(c). In Figs. 1(d) and 1(e) the tip of the induced counterclockwise spiral wave can be observed clearly. In the final state, only a counterclockwise spiral wave exists in the medium. After the illumination has been removed, the position of the induced spiral wave can shift in space, and therefore its final position does not exactly coincide

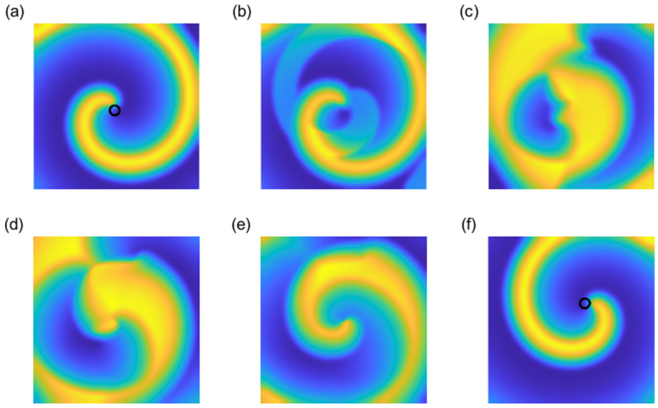

FIG. 1. The numerical simulation of Burton's experiment. The Barkley model of reaction-diffusion system is used. Parameters are $D = 1$, $a = 1.1$, $b = 0.19$, and $\varepsilon = 0.02$. Color coding shows the recovery variable v. Black solid lines represent the tip trajectory of the spiral waves. (a) The initial state shows a clockwise spiral wave. (b)–(e) A counterclockwise spiral-shaped light is applied to the medium. The angular frequency $\omega_L = 1.1\omega_0$, the light intensity $I_0 = 0.2/\Delta t$, and the illumination time duration $\delta = 1.5T_0$ are chosen. (f) The final state, where a counterclockwise rigidly rotating spiral wave remains in the medium.

with the position of the initial spiral wave or the light pattern. Applying a counterclockwise spiral wave as the initial condition and applying a clockwise rotating spiral-shaped light to the medium yielded the same result since the simulation medium was symmetric. We have repeated our simulations by changing the phase difference between the initial spiral wave and the light. Each trial resulted in successful reversal, which verifies that the reversal is independent of the phase difference. These results are consistent with the experiments in Ref. [20].

However, what the experiments show is not the reversal of the chirality of the original spiral wave, but the recreation of a spiral wave. This spiral wave is induced into the system, dominates the whole medium, and overwrites the previous wave. In other words, we are able to control the chirality of the system by recreating a spiral wave.

If we increase the illumination time duration δ with the other parameters unchanged, the spiral wave will be synchronized by the light and no more spiral waves will be recreated. If δ is less than a critical value of $0.9T_0$, the chirality control will fail.

Previously, methods for selecting the chirality of the spiral waves by applying an external chiral field were investigated [12,27]. Nevertheless, the selected spiral waves existed in the medium before the external field was applied.

B. Spiral recreation using spatial offset

To support our view, we give more details based on our model. First, we show that the spiral-shaped light with the same chirality as the existing spiral wave can accomplish the recreation. We put the center of the initial counterclockwise spiral wave on the diagonal of the medium, while the counterclockwise spiral-shaped light was located at the center of the medium. The process is shown in Fig. 2. Similar to

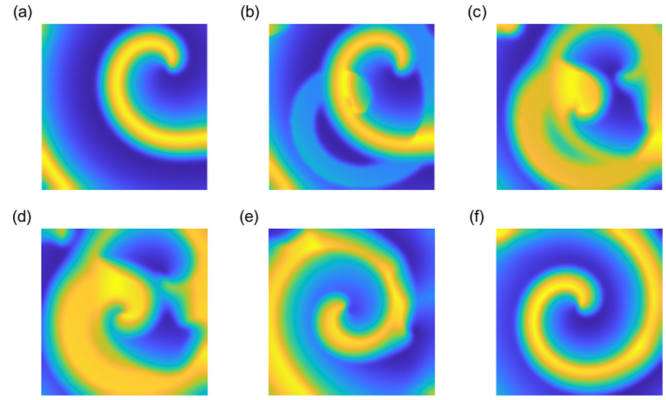

FIG. 2. Spiral recreation using spatial offset. Color coding shows the recovery variable v. Other parameters are the same as in Fig. 1.

Fig. 1(b), there is a spiral wave induced into the medium shortly after the illumination begins in Fig. 2(b). In Fig. 2(d) the tip of the induced spiral wave can be observed clearly. The original spiral wave disappears in Fig. 2(e). In the final state, only one spiral wave remains at the center of the medium. It seems that the initial spiral wave shifts to a different position with optogenetics, but in fact, a spiral wave was created and overwrites the initial spiral wave.

C. Illumination with a spiral-pair-shaped light

Figure 3 shows the simulation outcome when the illumination is in the shape of two rotating spirals of the same chirality. In this case, two spiral waves are created in Figs. 3(b)–3(e), and finally the system transforms into a double spiral system as shown in Fig. 3(f), implying that we can recreate not only the single spiral wave, but also other spatiotemporal patterns sustained by the medium.

D. Partial illumination

The dynamics of a spiral wave is often associated with the motion of the tip to some extent [28,29]. The phase of the neighboring elements of the tip determines the chirality of the spiral wave; see Ref. [30] and Eq. (1). We study if the partial illumination around the tip can control the spiral

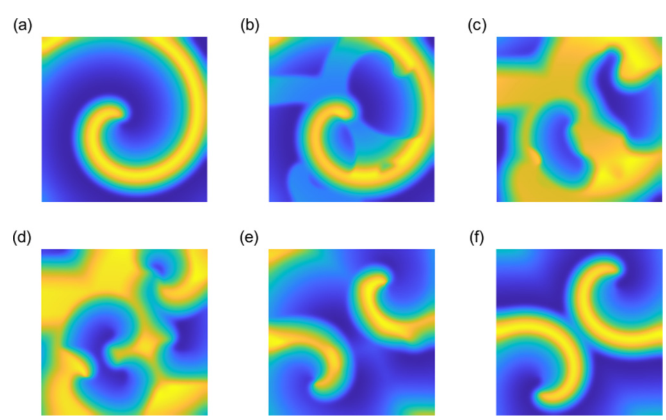

FIG. 3. Recreation of the spiral pair pattern. Color coding shows the recovery variable v. Other parameters are the same as in Fig. 1.

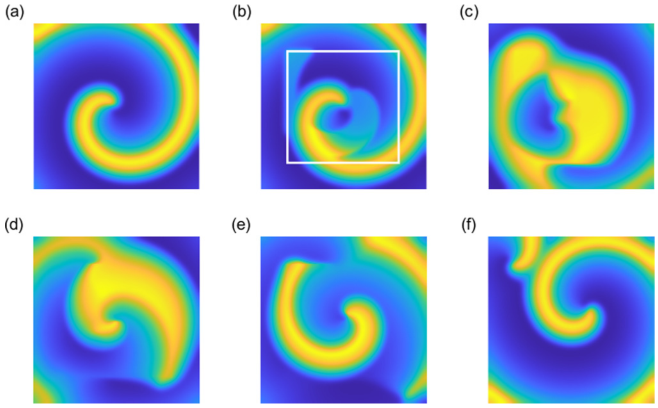

FIG. 4. A typical process showing the unsuccessful control of the spiral wave chirality by partial illumination. Color coding shows the recovery variable v. White box represents the illuminated region 16×16. Other parameters are the same as in Fig. 1.

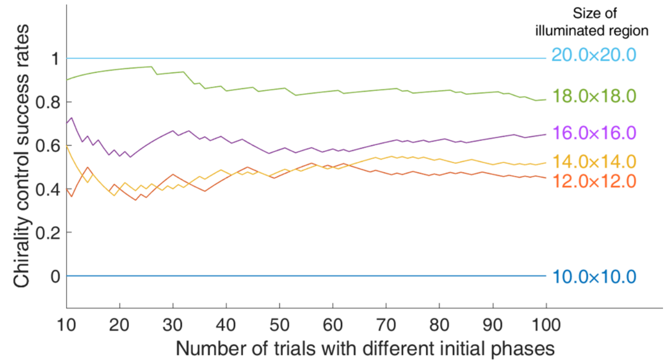

FIG. 5. Chirality control success rates with different illuminated regions. The initial phase difference between the spiral and the applied light is randomly generated in each trial. All illuminated regions locate at the center of the medium. Other parameters are the same as in Fig. 1.

wave chirality through recreation. Similarly to Fig. 1, we use a clockwise spiral wave as the initial condition and the rotating spiral-shaped light is counterclockwise. We then define a successful control if there is only one spiral wave with the same chirality as the light pattern that survives in the final state. An unsuccessful control by partial illumination is shown in Fig. 4. Illumination is applied only to the central 16×16 region [white box in Fig. 4(b)] for $1.5T_0$. In Fig. 4(b) one can observe a clockwise spiral wave together with a counterclockwise spiral wave in the medium. In Fig. 4(d), although the counterclockwise spiral wave is successfully recreated, it fails to dominate the whole medium compared with Fig. 1(d). The wave segments outside the illuminated region are not influenced and form another tip on the periphery, and thereby a different spiral wave occurs. After the illumination is removed, two spiral waves coexist in the medium as shown in Fig. 4(f).

We vary the phase difference between the spiral wave and the applied light from 0 to 2π, and we find that in some cases, the control may succeed. We repeat our simulations with random phase differences 100 times, and the chirality control success rates with different illuminated regions are illustrated in Fig. 5. It can be concluded that a larger illuminated area corresponds to a higher success rate. No successful control is observed if the area of the illuminated region is smaller than 10×10. The success rates maintain at 100% when the area is beyond the threshold area 20×20. Therefore, we believe that this kind of chirality control technique requires sufficient illumination area, preferably a global one.

E. Illumination on meandering spiral wave and multiple spiral wave systems

The tip motions of spiral waves found in natural systems are often meandering [14,31]. The meandering or drifting of spiral waves is mainly caused by the characteristics of the medium itself. Previously in Sec. III B we have revealed that the control of the spatiotemporal patterns is independent of the relative position of the applied light and the existing spiral wave. On this basis, we verify if our method is effective for meandering spiral waves. As shown in Fig. 6(a), we start with the initial condition where a meandering spiral wave rotates clockwise. In Figs. 6(b)–6(d) the global illumination succeeds to recreate a spiral wave. In the final state, only one spiral wave rotates counterclockwise in the medium.

So far, we have simulated the recreation and overwriting of the single spiral system through illumination. While spiral waves generated in living systems usually appear in pairs, suggesting that we sometimes have to face a system with more than one spiral wave. Next, let us consider the optogenetics in a medium with multiple spiral waves. We expand the medium area to 70×70 to accommodate more spiral waves. Figure 7 shows the effect of illumination on a multiple spiral wave system. As is illustrated in Fig. 7(a), both clockwise and counterclockwise spiral waves exist in the initial condition. A global illumination with a single spiral-shaped light is applied to the system during in Figs. 7(b)–7(e). As expected, the clockwise spiral wave is recreated and successfully overwrites the previous waves. Finally, only a clockwise spiral wave survives.

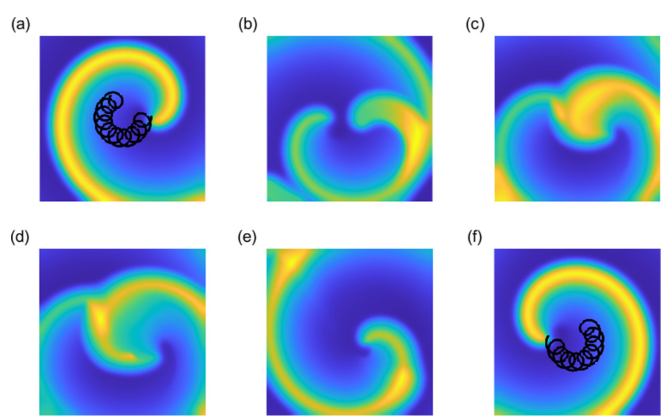

FIG. 6. The recreation of a meandering spiral wave chirality by the rotating spiral-shaped illumination. The angular frequency of the spiral-shaped light $\omega_L = 1.1\omega_1$ and the illumination time duration $\delta = 1.5T_1$. Color coding shows the recovery variable v. Black solid lines represent the tip trajectory of the spiral wave. Parameters are $a = 0.58$, $b = 0.05$, and $\varepsilon = 0.02$. Other parameters are the same as in Fig. 1.

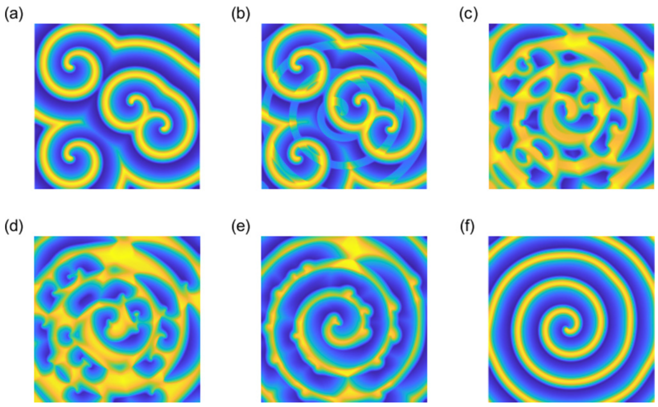

FIG. 7. The effect of a global spiral-shaped illumination applied to the multiple spiral wave system. Color coding shows the recovery variable v. System size is 70×70. (a) The medium consists of four spiral waves, including three counterclockwise spiral waves and one clockwise spiral wave. (b)–(e) A clockwise spiral-shaped illumination is applied to the medium. (f) The final state shows only one clockwise rotating spiral wave remaining in the medium. Other parameters are the same as in Fig. 1.

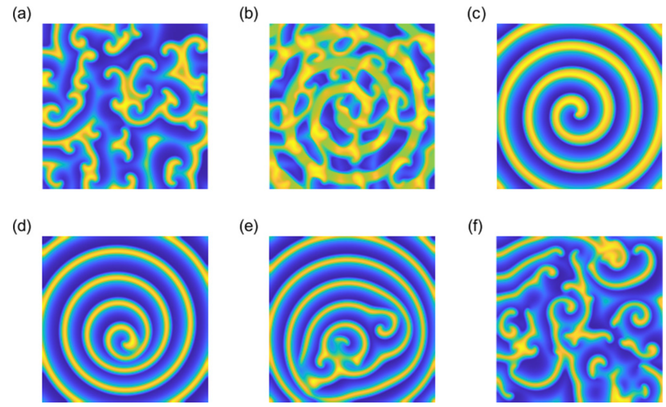

FIG. 9. Optogenetics control of the turbulent state with the Bär model. Parameters are $D = 1$, $a = 0.84$, $b = 0.07$, and $\varepsilon = 0.072$. Color coding shows the recovery variable v. System size is 70×70. The angular frequency of the applied light $\omega_L = 1.1\omega_3$ and the duration $\delta = 1.5T_3$ are chosen. (a) Initial state of spiral wave turbulence. (b)–(c) A clockwise spiral-shaped illumination is applied to the medium. (d)–(f) The evolution of the medium after the illumination stops. Other parameters are the same as in Fig. 1.

F. Resynchronization of turbulent systems

Inspired by the success of the overwriting of multiple spiral wave system, we then try to find the effect of global illumination with the rotating spiral-shaped light applied to the turbulent system. The variant of the Barkley model is used to create the turbulent state. An example is shown in Fig. 8. One can observe from Fig. 8(b) that a spiral wave is created in the medium which has no signs of breaking up. In Fig. 8(c) the induced spiral wave occupies the entire medium during illumination, and no spiral defects remain. Due to the parameters chosen in the system, the spiral wave begins to break up after the illumination stops as shown in Fig. 8(d). Finally in Fig. 8(f) the turbulent state is restored. Various simulations with different initial conditions show the robustness of our method.

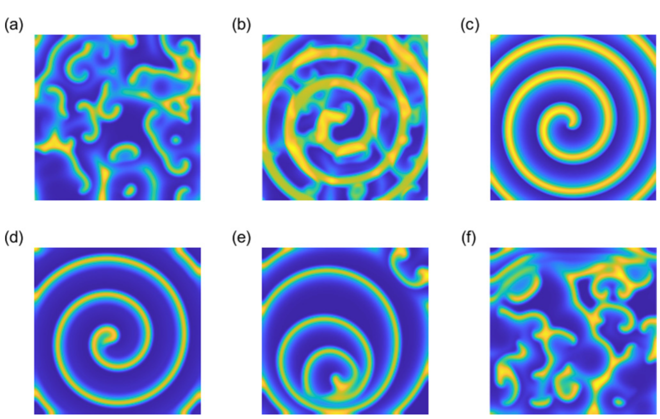

FIG. 8. Short-term resynchronization of turbulent state during rotating spiral-shaped illumination. The variant of the Barkley model is used. Parameters are $a = 0.6$, $b = 0.06$, and $\varepsilon = 0.0875$. Color coding shows the recovery variable v. System size is 70×70. The angular frequency of the applied light $\omega_L = 1.1\omega_2$ and the duration $\delta = 1.5T_2$ are chosen. (a) Initial state of spiral wave turbulence. (b)–(c) A clockwise spiral-shaped illumination is applied to the medium. (d)–(f) The evolution of the medium after the illumination stops. Other parameters are the same as in Fig. 1.

To further check to which extent the optogenetics method is model independent, we apply this method in the Bär model [26]. Figure 9 shows an example of optical control of turbulent state under the Bär model. It can be seen that the phenomenon is similar to that in Fig. 8. These results support the idea that the optogenetics control method is robust and model independent.

IV. DISCUSSION

In our study we have used a simplified generic description of the optogenetics current as an instantaneous inward current. More detailed descriptions of optogenetics currents have been formulated, e.g., via a Markov state model as in Ref. [19]. The Markov state model of a light-activated protein called channelrhodopsin-2 (ChR2) used in Ref. [19] was constructed on the basis of experimental data in Ref. [32]. The experiments showed that the typical activation time of the ChR2 channels is on the order of 2–5 ms, which is substantially shorter than a duration of action potential or period of spiral wave in the heart. As in our case typical optical stimulation was longer than the period of a spiral wave, we think that such a delay in activation can be neglected in our generic study. It would, however, be interesting to reproduce our studies in a more detailed model for cardiac tissue with a detailed description of the ChR2 channels to discover if additional details result in alternative qualitative effects.

In the human heart, the accurate location of the spiral wave during AF is hard to acquire due to the difficulty in obtaining spatiotemporally varying electrical activity. Although a high-resolution mapping technique using optical dyes has achieved in determining the complex wave organization of the extracorporeal human heart [33], it is still infeasible in *in vivo* heart because of the toxicity of the dyes [34]. Electrode separation techniques are able to provide a spatial resolution of only approximately 1–5 mm, which allows one to roughly identify the tip position of the spiral wave. In this sense, it is still technically difficult to let the center of the spiral-shaped illumination coincide exactly with that of the existing spiral waves *in vivo*. The simulations described in Sec. III B show that the recreation is not sensitive to the relative position of the spiral-shaped light and the existing spiral wave. This property will reduce the difficulty of controlling the spiral waves in the heart with optogenetics.

In Sec. III E a single spiral wave was recreated in the multiple spiral wave system through optogenetics. The number of the topological defects reduces from four to one after the illumination. Generally, it is more difficult to control a multiple spiral wave system than a single spiral wave system. Transforming a multiple spiral wave system into a single spiral wave system during AF in human heart can effectively simplify the process of finding the sources which sustain AF, thereby facilitating the treatment by ablation [35].

The instabilities of rotating spiral waves are known to underlie spatiotemporally chaotic dynamics, or turbulence, via spiral breakup [25]. During cardiac arrhythmias, the breakup of spiral waves in the heart develops ventricular tachycardia (VT) into life-threatening VF [36]. Currently, the most commonly used cardiac defibrillation method in clinical practice is to apply massive electrical shocks to heart, which may lead to irreversible damage to the heart muscle. Hence, a low-energy method for cardiac defibrillation is urgently needed. It has been demonstrated that controlling spiral turbulence in heart can effectively terminate fibrillation [37]. Turbulence suppression induced by an external field in the heart has been studied [38]. To date, a series of feedback and nonfeedback control methods have been proposed for suppressing turbulence [27,39–41]. In Sec. III F we find that optogenetics may temporarily resynchronize the turbulent system into a single spiral wave system. This may de-escalate the life-threatening VF to VT. Converting VF to VT around a self-chosen point is already one important step in low-energy defibrillation. Thus, our method of spatiotemporal control may provide a possibility for low-voltage heart defibrillation through optogenetics. Note, however, that its practical application would require expression of optogenetics channels in the heart of patients and a means to project light directly on the heart, which is highly nontrivial and a yet unsolved problem.

V. CONCLUSION

In summary, we have studied the recreation and chirality control of spiral wave patterns using optogenetics by numerical simulations. We used the classical Barkley model with a function $I(x, y, t)$ to represent the illumination. We first reproduced the experiments of the reversal of spiral chirality in Ref. [20] through numerical simulations, and we revealed that the mechanism of the experiments is the recreation of a spiral wave. Using this principle, we are able to control the spatiotemporal pattern of the medium through optogenetics. We showed the recreation of a spiral wave using spatial offset as well as the recreation of a spiral pair. We also demonstrated that the pattern control is independent of relative position and phase difference of the spiral-shaped light and the existing spiral wave, but sensitive to the area of the illuminated region. Meandering spiral waves can also be controlled. In addition, we found that a single spiral-shaped illumination can transform a state with multiple spiral waves into a single spiral wave system; it can also temporarily resynchronize the turbulent state. Our methodology has distinctive features. It achieves creating a desired spiral chirality which is absent in the initial state. Meanwhile, it can reduce the number of topological defects in a multiple spiral wave system or turbulent system, which is interesting since a single spiral wave is more easily controlled in biological systems. In cardiac electrophysiology context, a single spiral wave is more amenable to ablation therapy. The methodology presented is not model dependent, and thus it works for different reaction-diffusion systems. We hope that our methodology will be further tested and implemented in practical applications.

ACKNOWLEDGMENTS

This work was supported by the National Natural Science Foundation of China under Grant No. 12005066. Research at Sechenov University was financed by the Ministry of Science and Higher Education of the Russian Federation within the framework of state support for the creation and development of world-class research centers, "Digital Biodesign and Personalized Healthcare," No. 075-15-2020-926. We thank H. Zhang for valuable discussions.

[1] K. Tsuji and S. C. Müller, *Spiral and Vortices in Culture, Nature, and Science* (Springer, Cham, 2019).
[2] A. T. Winfree, Science **175**, 634 (1972).
[3] S. Jakubith, H. H. Rotermund, W. Engel, A. von Oertzen, and G. Ertl, Phys. Rev. Lett. **65**, 3013 (1990).
[4] J. Lechleiter, S. Girard, E. Peralta, and D. Clapham, Science **252**, 123 (1991).
[5] A. T. Winfree, J. Theor. Biol. **138**, 353 (1989).
[6] A. V. Panfilov, H. Dierckx, and V. Volpert, Physica D **399**, 1 (2019).
[7] F. X. Witkowski, L. J. Leon, P. A. Penkoske, W. R. Giles, M. L. Spano, W. L. Ditto, and T. Winfree, Nature (London) **392**, 78 (1998).
[8] J. Jalife, J. Cardiovasc. Electr. **14**, 776 (2003).
[9] T. Quail, A. Shrier, and L. Glass, Phys. Rev. Lett. **113**, 158101 (2014).
[10] M. Zhan, J. M. Luo, and J. H. Gao, Phys. Rev. E **75**, 016214 (2007).
[11] V. Zykov, A. Krekhov, and E. Bodenschatz, Proc. Natl. Acad. Sci. USA **114**, 1281 (2017).
[12] B. W. Li, L. Y. Deng, and H. Zhang, Phys. Rev. E **87**, 042905 (2013).
[13] L. Ji, Y. Zhou, Q. Li, C. Qiao, and Q. Ouyang, Phys. Rev. E **88**, 042919 (2013).
[14] O. Steinbock and S. C. Müller, Phys. Rev. E **47**, 1506 (1993).
[15] K. Deisseroth, Nat. Methods **8**, 26 (2011).

[16] P. Sasse, M. Funken, T. Beiert, and T. Bruegmann, Front. Physiol. **10**, 675 (2019).

[17] R. Majumder, I. Feola, A. S. Teplenin, A. A. F. Vries, A. V. Panfilov, and D. A. Pijnappels, eLife **7**, e41076 (2018).

[18] B. O. Bingen, M. C. Engels, M. J. Schalij, W. Jangsangthong, Z. Neshati, I. Feola, D. L. Ypey, S. F. A. Askar, A. V. Panfilov, D. A. Pijnappels, and A. A. F. Vries, Cardiovasc. Res. **104**, 194 (2014).

[19] S. Hussaini, V. Venkatesan, V. Biasci, J. M. R. Sepúlveda, R. A. Q. Uribe, L. Sacconi, G. Bub, C. Richter, V. Krinski, U. Parlitz, R. Majumder, and S. Luther, eLife **10**, e59954 (2021).

[20] R. A. B. Burton, A. Klimas, C. M. Ambrosi, J. Tomek, A. Corbett, E. Entcheva, and G. Bub, Nat. Photon. **9**, 813 (2015).

[21] D. Barkley, Physica D **49**, 61 (1991).

[22] J. X. Chen, H. Zhang, and Y. Q. Li, J. Chem. Phys. **130**, 124510 (2009).

[23] I. V. Biktasheva, D. Barkley, V. N. Biktashev, G. V. Bordyugov, and A. J. Foulkes, Phys. Rev. E **79**, 056702 (2009).

[24] T. C. Li, B. W. Li, B. Zheng, H. Zhang, A. Panfilov, and H. Dierckx, New J. Phys. **21**, 043012 (2019).

[25] M. Bär and L. Brusch, New J. Phys. **6**, 5 (2004).

[26] M. Bär, N. Gottschalk, M. Eiswirth, and G. Ertl, J. Chem. Phys. **100**, 1202 (1994).

[27] T. C. Li, X. Gao, F. F. Zheng, M. C. Cai, B. W. Li, H. Zhang, and H. Dierckx, Phys. Rev. E **93**, 012216 (2016).

[28] J. J. Tyson and J. P. Keener, Physica D **32**, 327 (1988).

[29] T. C. Li, D. B. Pan, K. S. Zhou, R. H. Jiang, C. Y. Jiang, B. Zheng, and H. Zhang, Phys. Rev. E **98**, 062405 (2018).

[30] N. D. Mermin, Rev. Mod. Phys. **51**, 591 (1979).

[31] D. T. Kim, Y. Kwan, J. J. Lee, T. Ikeda, T. Uchida, K. Kamjoo, Y. H. Kim, J. J. C. Ong, C. A. Athill, T. J. Wu, L. Czer, H. S. Karagueuzian, and P. S. Chen, Chaos **8**, 137 (1998).

[32] J. C. Williams, J. J. Xu, Z. J. Lu, A. Klimas, X. X. Chen, C. M. Ambrosi, I. S. Cohen, and E. Entcheva, PLoS Comput. Biol. **9**, e1003220 (2013).

[33] K. Nanthakumar, J. Jalife, S. Massé, E. Downar, M. Pop, J. Asta, H. Ross, V. Rao, S. Mironov, E. Sevaptsidis, J. Rogers, G. Wright, and R. Dhopeshwarkar, Am. J. Physiol. Heart Circ. Physiol. **293**, H875 (2007).

[34] W. J. Rappel and S. M. Narayan, Chaos **23**, 023113 (2013).

[35] S. M. Narayan, D. E. Krummen, K. Shivkumar, P. Clopton, W. J. Rappel, and J. M. Miller, J. Am. Coll. Cardiol. **60**, 628 (2012).

[36] E. B. Bourgeois, H. D. Reeves, G. P. Walcott, and J. M. Rogers, Cardiovasc. Res. **93**, 272 (2012).

[37] S. Sinha, A. Pande, and R. Pandit, Phys. Rev. Lett. **86**, 3678 (2001).

[38] S. Luther, F. H. Fenton, B. G. Kornreich, A. Squires, P. Bittihn, D. Hornung, M. Zabel, J. Flanders, A. Gladuli, L. Campoy, E. M. Cherry, G. Luther, G. Hasenfuss, V. I. Krinsky, A. Pumir, R. F. Gilmour Jr, and E. Bodenschatz, Nature (London) **475**, 235 (2011).

[39] H. Zhang, B. B. Hu, and G. Hu, Phys. Rev. E **68**, 026134 (2003).

[40] S. Sridhar and S. Sinha, Europhys. Lett. **81**, 50002 (2008).

[41] T. C. Li, B. Q. Ai, Y. Chen, and B. W. Li, Phys. Lett. A **388**, 127058 (2021)